Initial Investigation into UAV Application of a Biomimetically Derived Span-Wise Morphing Structure

Benjamin J. Stacey* and Peter R. Thomas.†
University of Hertfordshire, Centre for Engineering Research, College Lane, Hatfield, Hertfordshire, AL10 9AB, United Kingdom

Presented in this paper is the initial evaluation of a span-wise morphing concept for UAV applications. The dynamic response is investigated via a method of external photogrammetry taken of the wing concept structure. A process of metrology is undertaken to ascertain the effective displacement of the wing tip undergoing a large span and chord-wise morphing actuation, based on a biomimetically inspired joint mechanism driven through pneumatic artificial muscles. A static case is employed to ascertain the repeatability of the morphing geometry in relation to the commanded position and to an derived average actuation position. This is repeated under a simulated aerodynamic loading for a UAV application. A dynamic case is also evaluated for the concept in relation to the proposed aircraft application. The resulting dynamic response is also compared to the similarly dynamic response observed in the avian from which the concept is derived.

I. Introduction

Biomimicry is commonly found at the forefront of modern engineering design. This is perhaps most true for the development of small unmanned aerial vehicles where aeronautical design is unrestricted from traditional constraints. Unmanned vehicles have also served as the platform on which to prove such concepts for integration into piloted platforms [1]. Subsequently, the number of biomimetically derived concepts has increased. The reasons are perhaps obvious: the opportunity to improve efficiency through material and surface optimization [2] [3], increased performance via improved control authority [4] and bio-inspired flight profiles, amongst others [5] [6]. In this paper the development of a biomimetic UAV concept will be approached from the field of morphing structures. These structures allow the alteration of the aerodynamic shape of the vehicle on-mission to suit the flight regime. When applied to the wing of an aircraft advantages can range from reduced drag to increased stability or control and it is an area with a significant number of morphing concepts. Presented here is the application of a span-wise morphing concept as the basis for the structure of a small unmanned aerial vehicle. In this paper the structure is optimized through the study of macro-structural avian anatomy. The lifting surface morphing is then achieved via pneumatic artificial muscles (PAMs) and the performance characterized in reference to a UAV application.

When considering the application of a morphing structure in the airframe of a proposed aircraft one of the primary specifications relates to the consistency of the structures deflection. This is perhaps more acute when related to morphing lifting surfaces. The geometry of the lifting surface directly effects to the dominant aerodynamics forces generated and therefore so does, by extension, any morphing. Obviously, this is the intension in most concepts and so the change in aerodynamic forces is desired. However, with any controlled system there is a steady state error. This can arise from the control itself or the structure, both of which therefore need to be quantified for the application of any proposed concept. The compliant nature of actuated structures typically results in a structure with reduced stiffness. However, this is not given and particularly in recent proposed system concepts this reduced stiffness may only be present in a single axis thus allowing for it is be compensated with other structural elements. However, there is still an increased emphasis on aeroelastic effects [7] as a result of this lower stiffness. It maybe considered that the primary mechanism for precise repeated motion is the driving actuations system. Pneumatic artificial muscles are continually considered for morphing concept applications in UAS [8]. While more commonly applied industrially in manufacture and robotics a high specific strength has resulted in suitability for morphing structures where reduced weight at the point of use, such as a structure in motion, is desirable. Typical of actuation development much has been discussed in the modelling and control of these actuators. Literature has also investigated reliability and fatigue characteristics [9]. Similarly, predictive methodologies have been developed to assess the accuracy of the PAM based actuation system in a morphing

*Senior Lecturer, School of Physics, Engineering, and Computer Science, College Lane, Hatfield, Hertfordshire, AL10 9AB, United Kingdom
†Principal Lecturer, School of Physics, Engineering, and Computer Science, College Lane, Hatfield, Hertfordshire, AL10 9AB, United Kingdom

lifting surface [10]. This employed fibre Bragg grating sensors to monitor PAM deflection which is not applicable in a joint actuation system such as the span-wise morphing concept. However, it is clear the aerodynamic loading cannot be neglected. Similar, large surface area deflecting lifting surface concepts have been evaluated with respect to these dynamic forces [11]. In particular, a case of a Z-shaped structure exhibiting a span motion coupled with an out-of-plane motion similar to a gull-wing. The structure was evaluated via simulation whereby the motion of the structure was modelled via a Craig–Bampton vector synthesis method. The aerodynamic forces subsequently derived via an unsteady vortex lattice method. Proven to be an effective holistic methodology this does not, however, represent the minor perturbations inherent in an imperfect mechanism.

The span-wise morphing concept consists of three linked members analogous to the skeletal structure of the avian wing [12]. Each joint exhibits one degree-of-freedom, on the same plane, providing the end effector three degrees of freedom. In this instance the end effector relates to the wing tip, as such providing the concept with lateral span and chord motion in addition to rotation about the vertical axis resulting in an effective wing sweep. The motion of the concept is under-constrained and so an effective relation between the joints is required. While a simple ratio is considered for the concept it is found that the avian, from which the linked members are derived, does not exhibit this motion. Analysis of avian motion capture data indicates an interrupted joint rotation for the extension of the wing structure. This forms the bases of a UAV system designed for effective span-wise control of the lifting surface. The structure impacts the aerodynamic and stability characteristics of any proposed aircraft into which it is incorporated. The joint relationships and the effectiveness of their actuation therefore play a significant role in achieving increased effective aircraft control. Particularly, in the structure's dynamic response to span changes in flight where the lifting surface itself is applied to affect control in roll and pitch.

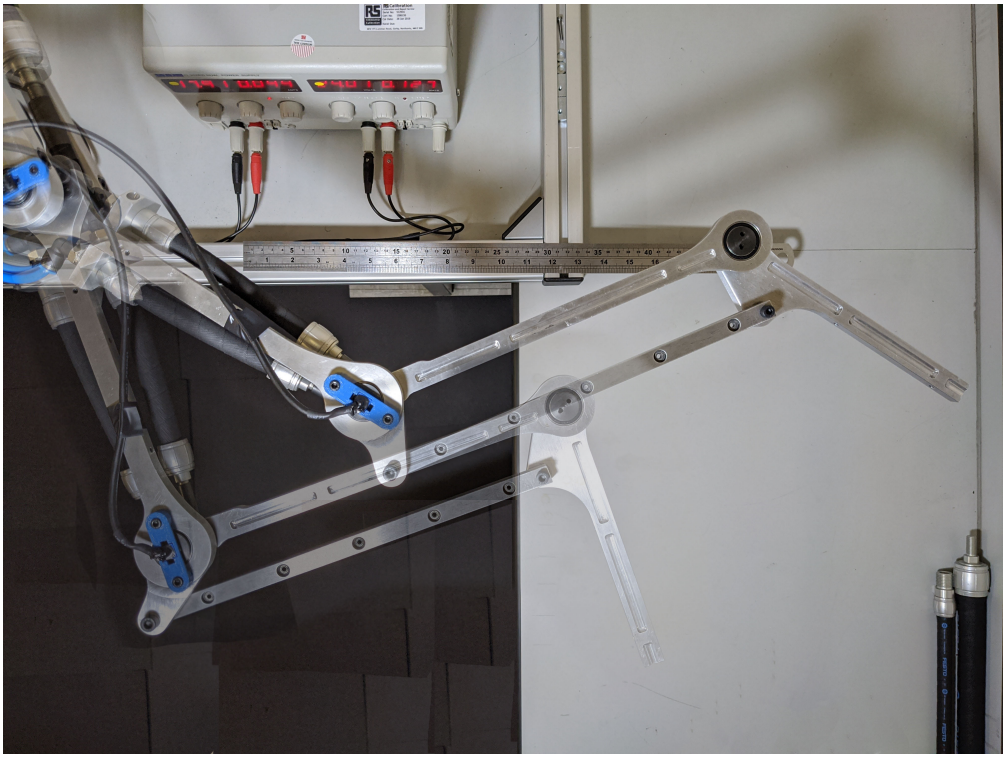

Fig. 1 Span-wise morphing structure in a fully extended position and retracted overlaid. Each pneumatic artificial muscle (PAM) antagonistic pair is visible actuating each respective joint.

The proposed wing structure utilizes this concept for an internal driven skeleton, shown in figure 1. The member lengths impact the morphing performance of the structure. To achieve a lifting surface area change sufficient to impact the performance of the vehicle a study was conducted into the avian skeleton on which the concept was based. Data collected and collated [13] was applied in an optimization process to produce member lengths for the structure. This morphing structure was subsequently manufactured. Pneumatic artificial muscles actuated both the analogous 'shoulder' and 'elbow' joints though an antagonistic bell-crank mechanism. The motion captured relation between the three joints

was applied to the structure. The pneumatic muscles themselves are presented and sized to reproduce both the simple ratio and biomimetically derived motion. Mechanical geometry is also assessed as a contributing factor to the motion and the wrist actuation via a parallels mechanism is further developed in relation to the biological captured motion. However, the aspect with the greatest effect on the structures motion is the specification of the pneumatic system. These contributing factors are presented and applied as variables in the structures performance.

The structure achieved an angular range of motion of 45° and 30° in the 'elbow' and 'shoulder' joints respectively. A process to determine the deflection of the wing structure was undertaken. The contributing variables to the motion of the structure independently analyzed as to the impact on the performance of the structure. Photogrammetry and static laser 3D scanning produced an evaluation of the prototype in terms of span and area morphing percentage. As well as factors resulting from the two joint motion types such as deformation under load and morphing consistency. Overall, a 38% span reduction was observed in line with similar concepts and the original span-wise morphing concept. While the biomimetically derived motion of the joints found to contribute to the reduction in out-of-plane deformation in the dynamic response of the structure.

II. Position Experimental Setup

Stereo-photogrammetry based metrology was the measurement technique employed as the external validation tool for the morphing concept. The concept being static resulted in a more repeatable setup across span-wise actuations. Thus increased precision could be achieved via a visual measurement system as opposed to range finding systems producing point clouds. Visual-based metrology can also exhibit a measurement rate in excess of $2x10^5$ Hz providing insight into the dynamics of the objective system. Two Photron Fastcam Mini UX50 cameras were mounted together to provide the stereo-setup; at an angle from normal plane of the subject of 12.5°. These were triggered simultaneously and synchronised through all recordings. As the cameras were static and frames taken synchronously only a single calibration was required to adjust for discrepancies in the rig and lenses. Fixed prime 100 mm lenses were setup fully closed down at an F24 aperture, providing the greatest depth-of-field possible for this system. Increased depth-of-field in this instance ensured points of interest on the concept that were set-back from the focal plane did not become unfocused decreasing accuracy in determining position. At a stand-off distance of 606 mm the controlled volume comprised 40 mm x 50 mm x 50 mm. A small volume as used here provides the resolution required to distinguish both the hysteresis and small perturbations immediately following the concept actuation. It was therefore employed for capture of the structure outboard point, which can determine the true pose of the system via the same kinematics/inverse kinematics which drive the joints. To provide contrast in the surface of the material high contrast markers were positioned on the end of the outboard member. These were black and white two dimensional paper marks as it is the contrast between the colours that is tracked as opposed to the colour or marker material itself. These are labelled in figure 2 along with the cameras as configured for the tests looking a the wing tip.

Alongside the static and dynamic performance of the morphing concept alone it was considered necessary to identify the positional performance of the concept while loaded. As stated previously the pose of the concept impacts the platform area of the lifting surface. While it is tempting to treat this dependency as proportional the nature of the aerodynamic surfaces to cover the concept result in a relationship difficult to quantify outside of the wind tunnel. The overlapping or morphing surface components result in both span-wise and out of plane geometric changes which are not consistent across the full span change. There is therefore potential for this to be highly non-linear and potentially dependent on uncontrolled variables. Temperature effecting the elasticity of flexible polymers is one example of an uncontrolled variable which could significantly vary change the lift produced by the surface across different span extensions. A mitigatory process for the impact of these differences in pose is to quantify the likely deviation under the aerodynamic load. However the difficulty presented here is in simulating the load. While the ideal case would be to aerodynamically load the model using an intended lifting surface this presents an issue in measurement. Any lifting surfaces considered for the concept would obscure the internal members resulting in position measurements being obviated to the surface itself. While applicable this would not allow a distinction to be made as to the base structure's repeatable motion. Static loading was therefore achieved via weights distributed across the structure. Point masses were applied on each structural member representing the distributed load transferred to that section of structure through the lifting surface. A setup of cradles and load actuators was considered, however, discounted as the actuation of the concept made consistent distribution of the load not viable. Applied weights for simulating loading has the notable disadvantage of affecting the system inertia. As a result no dynamic testing was conducted under simulated load.

The concept test rig consists of the span-wise morphing concept rigidly affixed to an extrusion frame in turn bolted to the measurement reference ground. While under simulated static load the concept was inverted. The reference axis

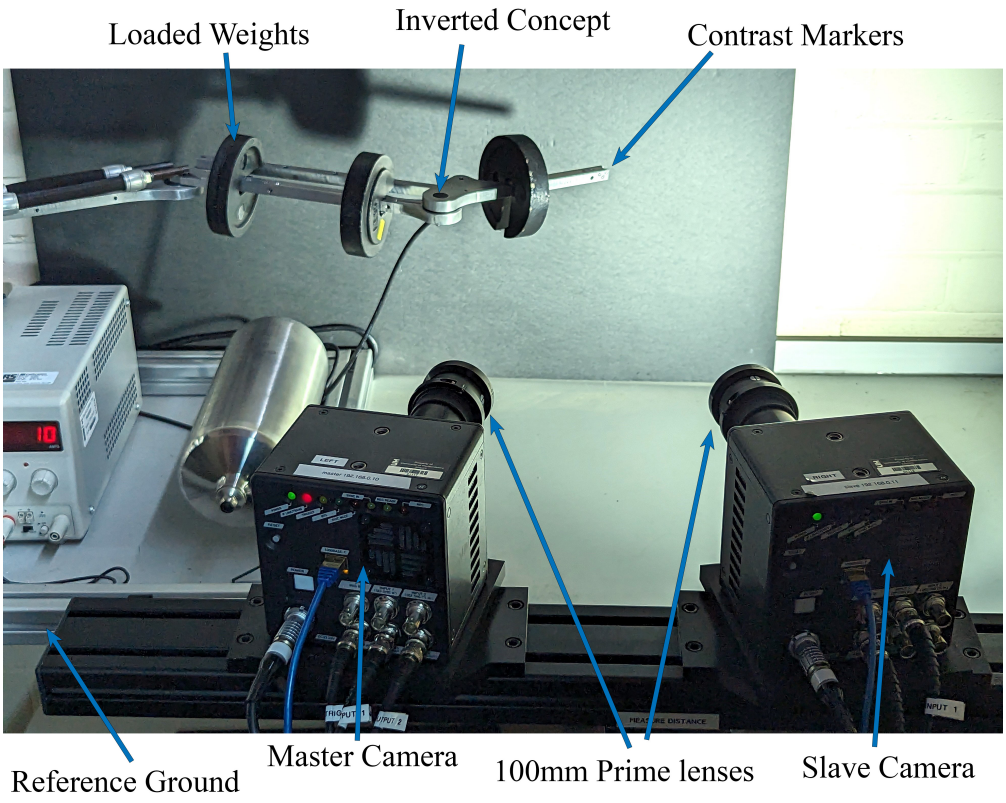

Fig. 2 The stereo high-speed camera setup shown with the simulated morphing concept loading. These cameras were run at 500 Hz and configured here to track the wing tip position within a capture volume of 40 mm x 50 mm x 50 mm. Visible on the concept are contrasting white and black markers this contrast allowing increased accuracy in identifying the concept's position.

was set via the model positioning. The span axis was set by ensuring the aluminium extrusion of the concept and camera rig were parallel. As the pneumatic artificial muscles (PAMs) are rigidly set at their respective angles in relation to this extrusion the span motion is by default aligned, thus the cameras are set too. This axis is set level via reference to a laser level. The longitudinal axis along the concept fuselage was not mechanically fixed and therefore exhibited a quantifiable error. This was adjusted by re-alignment within the meteorology post-processing software. However, it should be noted that this was achieved via use of the markers themselves. Three markers on one face of of the concept, shown in figure 3, were setup for this purpose. The assumption was made that the component surface, on which these markers were adhered, were vertical and parallel with aforementioned laser level thus ensuring the span-chord and span-out-of-plane planes were perpendicular. While, this was brought to within an acceptable tolerance this could not be measured and so the error is not quantified. This was also considered the largest source of error in the measurement process due the systematic nature of the camera and related software. An angular error of $\pm 0.5°$ was therefore taken representing the maximum machining error in the part. However, it should be noted this applied exclusively to the axis displacement results which are derived from the overall displacement which itself is not included in this assumption.

Calibration was the term given by the software for the process of removing lens and angle distortion. This also included the photogrammetric process of calculating the unknowns in each projected view of the cameras. Commonly completed in more manual photogrammetry with a chequerboard pattern of known dimensions this was not used in this case. A coded board was used, that is a board with coded shapes identifiable via computer vision. The industrial metrology software used recalled the required known physical dimensions based on this code unique to each size of calibration board. This is known to reduce systematic error often found in the process of photogrammetry as the positioning and interpretation of calibration objects is subjective.

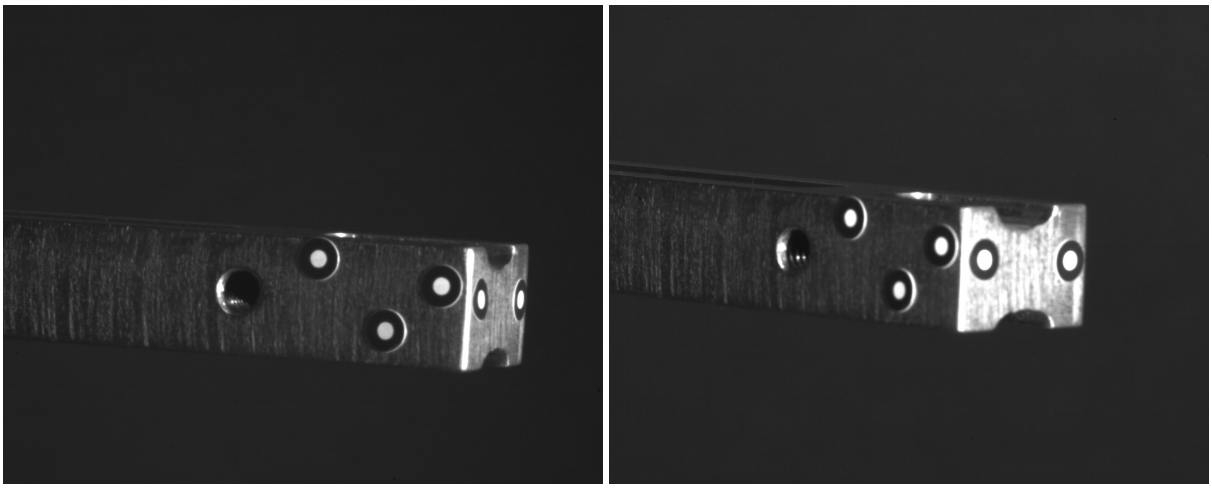

Fig. 3 Left and ring camera views as calibrated for the wing tip measurement volume. Each view depicts the wing tip in the non-inverted orientation, as taken unloaded, with the contrast markers in place.

III. Concept Precision

To characterise the concept's ability to repeat a retraction and extension cycle the end-point was measured in reference to a starting position. This initial position represents the PAMs being brought to their extended configuration from a depressurised state. Whilst allowing the difference in start-up and normal cycle behaviour to be identified, this also provided a reference position from which to measure defection of subsequent cycles. A value for deflection could then be ascertained from the average values measures across the five tracked points on the concept for each cycle. Via the process of photogrammetry the total displacement is derived from the angels measured in the projected view. Thus, the global coordinate position of the markers in cycle must be found from this and in reference to the aligned axis. As presented in table 1 where the x axis represents the span-wise direction, y out-of-plane, and z the longitudinal axis.

To obtain a representative sample the concept was set via a previously developed position control system, to target a dynamic sinusoidal wing span length. This allowed the a set of post-cycle positions to be collected within a single camera save and remove the chance to average dissimilar data. The sine frequency was set at 1 rad/s with the cameras triggered via this system at the peak/maximum extension. Due to camera hardware limitations the sample size was 500 cycles. Mean averages derived from the unloaded sample are presented in table 1 with the overall average displacement of 1.2656 mm. Representing 0.14% chord length of the concept this is indicative of a repeatable span-wise morph. Notable is the distribution of displacement magnitude across the components. The axis out-of-plane dy exhibits the least deviation across the sampled cycles and similarly shows the lowest maximum measured deviation of 0.3973 mm. This is the axis along which the concept has no intended motion so this is perhaps expected. As part of the joint mechanisms within the span-wise morphing concept the the joints contain disc springs designed to resist motion in this axis. Arguably the more significant direction of motion is dx the span-wise motion which showed a mean average deviation approximately half the overall displacement and 0.07% of the semi-span length. However, the maximum represents 0.13% deviation as a percentage of semi-span and given the distribution the cycle on which these present is essentially random. A span difference between the two semi-spans must therefore be considered to be a maximum 0.27%.

In the case where dz = 1.0393 mm that is the longitudinal axis in line with the body of the concept aircraft. It can be determined that the axis exhibits a increased deflection over dx when related to the intended motion in line. The chord motion of the wing tip is directly related to the span via the aforementioned biomimetic extension control for the concept. Dependent on PAM actuation pressure the chord motion can be approximated for this series of cycles as 200 mm. The resultant relative error in repeated position is 0.52%. It is arguable that this is not a direct comparison, however, it highlights the difference in accumulated error in the actuation system. It is hypothesised that the error in this axis is due to the primary joint responsible for the dz being the 'shoulder' joint; the inboard joint. This with an increased moment to the centre of mass could result in this noticeably higher position error.

The displacement in the loaded quasi-static case is similar with values representing an insignificant change over

those observed on the unloaded concept structure. These are summarized in table 2. The overall trend in these values does represent an increase in position error. The most significant of which is in the maximum deflection for the y out-of-plane axis approximately doubling. As this is the loading axis this is perhaps as expected but still leaves the position error for the axis in relation to the span motion at 0.1%.

It was noted in avian kinematics experimentation, summarized in previous literature [12], the apparent un-importance that motion in the dz axis is regarded in the behaviour of avian wings. In the span extension of avian wing an overshoot was observed, ranging up to 23.2% of the overall joint angular motion during span extension. It was concluded that this typically negative feature of dynamic response was offset by the decrease in rise time it facilitated in the span axis.

The dynamic response is plotted in a series of plot under figure 4. The aforementioned z axis motion here exhibits the overshoot found in the avian motion. The overshoot is not as significant as observed in the biological wing at approximately 2 mm or 0.2% as opposed to 23.3%. This leads to the conclusion that the concept is currently underperforming in terms of rise time and time to steady state. This would seem to suggest that the concept is too conservative in its performance at the detriment of dynamic response.

Table 1 Wing tip displacement observed in the unloaded concept across n = 500 cycles. Span-wise morphing concept was actuated as pressurised at 6 bar. Displacement in in reference to an initial position

Displacement Direction	Minimum (mm)	Maximum (mm)	$\bar{x}$ (mm)	σ (mm)
d	0.2047	2.5603	1.2656	0.5735
dx	0.0507	1.3270	0.6040	0.2727
dy	0.0013	0.3973	0.1700	0.1630
dz	0.0047	2.1847	1.0393	0.6533

Table 2 Wing tip displacement observed in the loaded concept across n = 500 cycles. Span-wise morphing concept was actuated as pressurised at 6 bar. Displacement in in reference to an initial position

Displacement Direction	Minimum (mm)	Maximum (mm)	$\bar{x}$ (mm)	σ (mm)
d	0.2137	2.6660	1.2373	0.5253
dx	0.0230	1.2193	0.7125	0.3398
dy	0.0133	0.9067	0.3451	0.2320
dz	0.0767	2.5467	0.8575	0.5249

IV. Conclusion

The dynamic response for the span-wise morphing concept is evaluated under simulated static aerodynamic loading. The concept is prototyped with structural members forming the basis of the morphing actuation system. This actuation is measured both for a quasi-static position and dynamic displacement via external photogrammetry based metrology. The morphing concept exhibits actuation in both the span and chord axes. This is achieved through a three jointed mechanism analogous to an avian wing. Actuation of the two inboard joint is affected by an antagonistic pair of pneumatic artificial muscles (PAMs) acting to produce am angular displacement.

In the quasi-static case is presented for both the unloaded and a static aerodynamic loading case. The wing tip position of maximum extension is evaluated for change in displacement over consecutive morphing cycles. These cycles represent a significant span reduction and extension. It was observed over a series of 500 cycles that the concept presented a maximum displacement of 0.28% the extended semi-span length. Perhaps of more note this the maximum deviation in the span axis directly impacting the primary direction of intended morphing. This value for deviation was found to be 0.07% the semi-span. Considered negligible in terms of direct effect on planform area. However, it is noted that any indirect effect on aerodynamic performance such as impact on pressure distribution is not considered in this evaluation; further characterisation is required.

The dynamic case is presented for only the unloaded but not the static aerodynamic loading case. It is noted that the simulated static loading is not suitable for a dynamic evaluation. It is proposed that this would require computational simulation as any physical method for applying a dynamic load would not be feasible with this amount of concept

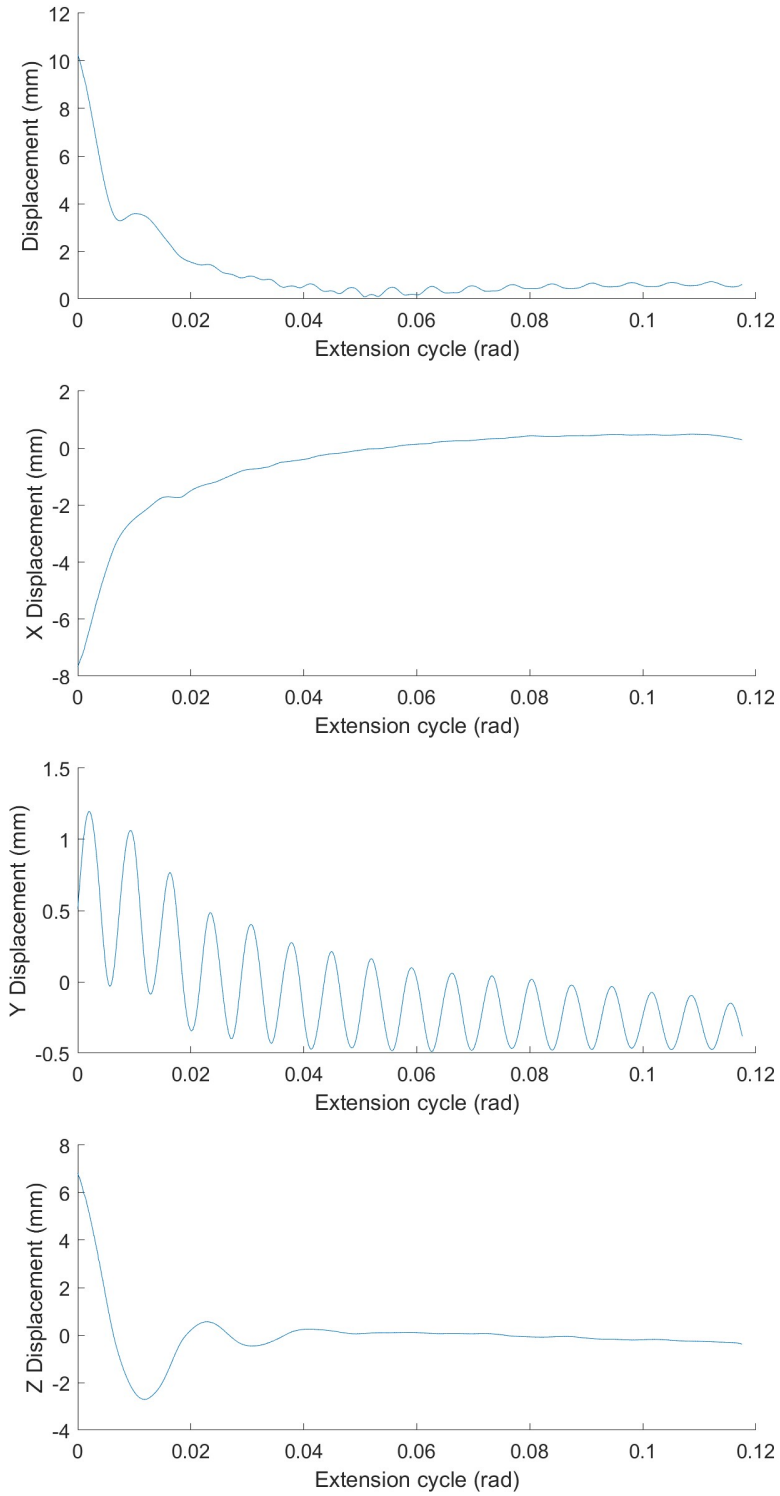

Fig. 4 The dynamic system response at the approach to and at full extension during a 1 rad/s sinusoidal span position input. Plotted against the extension cycle angle where the datum represents 1 rad from the input signal for maximum extension.

motion. In comparison to the avian motion data from which the concept is derived it is concluded that the concept is underperforming, that is to say the conservative errors in the response could be increase to improve position response in relation to time.

Acknowledgments

The authors would like to acknowledge the contributions to this research from the Sir Geoffrey De Havilland Fund.

References

[1] Sun, J., Guan, Q., Liu, Y., and Leng, J., "Morphing aircraft based on smart materials and structures: A state-of-the-art review," *Journal of Intelligent Material Systems and Structures*, Vol. 27, No. 17, 2016, pp. 2289–2312. https://doi.org/10.1177/1045389X16629569.

[2] Pennycuick, C. J., "Power requirements for horizontal flight in the pigeon columba livia," Vol. 49, 1968, pp. 527–555.

[3] Tobalske, B. W., "Biomechanics of bird flight," *Journal of Experimental Biology*, Vol. 210, No. 18, 2007, pp. 3135–3146. https://doi.org/10.1242/jeb.000273.

[4] Biewener, A. A., "Muscle function in avian flight: achieving power and control," *Philosophical Transactions of the Royal Society of London B: Biological Sciences*, Vol. 366, No. 1570, 2011, pp. 1496–1506. https://doi.org/10.1098/rstb.2010.0353.

[5] Taylor, G., Bacic, M., Bomphrey, R., Carruthers, A., Gillies, J., Walker, S., and Thomas, A., "New experimental approaches to the biology of flight control systems," *The Journal of Experimental Biology*, Vol. 211, 2008, pp. 258–266. https://doi.org/10.1242/jeb.012625.

[6] Shepherd, S., and Valasek, J., "Modeling and Analysis of Eagle Flight Mechanics from Experimental Flight Data," 2012. https://doi.org/10.2514/6.2012-27.

[7] Lee, D. H., and Weisshaar, T. A., "Aeroelastic on a folding wing configuration," *Collection of Technical Papers - AIAA/ASME/ASCE/AHS/ASC Structures, Structural Dynamics and Materials Conference*, Vol. 4, 2005, pp. 2452 – 2464.

[8] Zhao, S., Li, D., Zhou, J., and Sha, E., "Numerical and Experimental Study of a Flexible Trailing Edge Driving by Pneumatic Muscle Actuators," *Actuators 2021, Vol. 10, Page 142*, Vol. 10, 2021, p. 142. https://doi.org/10.3390/ACT10070142.

[9] Straka, L., "Operational reliability of mechatronic equipment based on pneumatic artificial muscle," *Applied Mechanics and Materials*, Vol. 460, 2014, pp. 41 – 48. https://doi.org/10.4028/www.scientific.net/AMM.460.41.

[10] Li, P., Liu, Y., and Leng, J., "A new deformation monitoring method for a flexible variable camber wing based on fiber Bragg grating sensors," *Journal of Intelligent Material Systems and Structures*, Vol. 25, 2014, pp. 1644 – 1653. https://doi.org/10.1177/1045389X13510220.

[11] Changchuan, X., Zhiying, C., and Chao, A., "Aeroelastic Response of a Z-Shaped Folding Wing During the Morphing Process," *AIAA Journal*, Vol. 60, 2022, pp. 3166 – 3179. https://doi.org/10.2514/1.J061138.

[12] Stacey, B. J., and Thomas, P. R., "A Biomimetically Derived Method for Control of Span-Wise Morphing Wings," *AIAA Science and Technology Forum and Exposition, AIAA SciTech Forum 2022*, 2022. https://doi.org/10.2514/6.2022-1986.

[13] Otto, C., "Comparative Morphological studies on detached bones [Translated]," 1981. URL http://www.palaeo.vetmed.uni-muenchen.de/download/dissertationen/otto_1981_accipitridae.pdf.